Original Article

Vajira Med J
Journal of Urban Medicine

Scattered Radiation Dose and Safety Assessment from Mobile X-Ray Radiography

Khwanpicha Chidtakhob BSc[1], Tharitsanat Amnakmanee BSc[2], Wasin Laesan BSc[2], Panatsada Awikunprasert PhD[3], Thunyarat Chusin PhD[4]

[1] *Division of Diagnostic Radiology, Faculty of Medicine Vajira Hospital, Navamindradhiraj University, Bangkok 10300, Thailand*
[2] *Bachelor of Science in Radiological Technology, Faculty of Medicine Vajira Hospital, Navamindradhiraj University, Bangkok 10300, Thailand*
[3] *Department of Radiological Technology, Faculty of Medicine Vajira Hospital, Navamindradhiraj University, Bangkok 10300, Thailand*
[4] *Department of Radiological Technology, Faculty of Allied Health Sciences, Naresuan University, Phitsanulok 65000, Thailand*

ABSTRACT

OBJECTIVE: This study aimed to measure the scattered radiation levels that surround a mobile X-ray machine during chest radiography using adult and pediatric phantoms and to estimate the radiation exposure experienced by nearby individuals in simulated clinical ward settings.

METHODS: Scattered radiation was measured using a solid-state scatter probe at distances of 1.0, 1.5, and 2.0 meter (m), and at nine angular positions around the X-ray tube. Chest X-ray (CXR) exposures were performed using two parameter sets: 80 kilovoltage peak (kVp) and 2 milliampere-seconds (mAs) for the adult phantom, and 55 kVp and 1.6 mAs for the pediatric phantom. The data obtained regarding the dose were used to simulate and calculate the potential scattered radiation exposure in hospital wards under three different scenarios: (1) without walls or shielding, (2) using measured distances based on the experimental setup, and (3) with shielding barriers, incorporating attenuation coefficients for common building materials.

RESULTS: For the adult phantom, the highest scattered dose was 0.26 microgray (μGy) at 1.0 m and the lowest was 0.03 μGy at 2.0 m. For the pediatric phantom, values ranged from 0.107 μGy to 0.002 μGy. The calculations of radiation dose using ward layouts showed that the annual exposure to adjacent patients and health care workers, based on 730 imaging sessions per year, did not exceed the International Commission on Radiological Protection annual public dose limit of 1 millisievert.

CONCLUSION: Scattered radiation levels during mobile CXR procedures decrease with distance and remain within safe limits. However, the cumulative low-dose exposure may contribute to long-term stochastic risks. Measures to protect against radiation, such as maintaining a minimum 2-m distance and wearing lead aprons, are recommended for safety.

KEYWORDS: inverse square law, mobile X-ray, radiation attenuation, scatter probe, scattered radiation

Corresponding author: Panatsada Awikunprasert, panatsada@nmu.ac.th
Received: 8 May 2025
Revised: 19 August 2025
Accepted: 9 September 2025
Vajira Med J 2025;69(4):e274832
http://dx.doi.org/10.62691/vmj.2025.274832

This work is licensed under a Creative Commons Attribution-NonCommercial-NoDerivatives 4.0 International License.

INTRODUCTION

For critically ill patients or those who cannot be transported to the X-ray department, mobile or portable X-ray radiography is particularly valuable. It also helps to reduce disease transmission during outbreaks such as COVID-19[1]. Portable chest X-rays (CXRs) are commonly used to assess lung and chest cavity abnormalities, monitor treatment progress, and evaluate preoperative conditions. However, CXRs use ionizing radiation, which can ionize atoms in its path, including the human body, thus exposing nearby staff members (radiographers, nurses, other health care workers) as well as patients to scattered radiation. Studies have shown that the intensity of the scattered radiation from portable X-ray machines decreases with distance from the patient and the use of radiation shielding[2,3]. In addition, scattered radiation levels are influenced by imaging parameters such as kilovoltage and milliampere-seconds (mAs)[3,4]. Unlike standard X-ray rooms, mobile X-ray units lack fixed protective barriers. During mobile CXR procedures, operators often need to stand close to patients to ensure proper positioning and to monitor factors such as respiration. In clinical practice, mobile X-ray is frequently performed in high-occupancy inpatient wards, intensive care units, and isolation rooms, where both health care workers and adjacent patients may remain in close proximity to the imaging area. These ward conditions, characterized by limited space and the presence of multiple individuals near the radiation source, can increase the likelihood of scattered radiation exposure. Although research suggests that the scattered radiation dose received by radiographers during CXRs is generally within safe limits[5], prolonged or repeated exposure without adequate protection could pose a long-term health risk to health care workers.

Scattered radiation can be measured by determining the air kerma using gas-filled detectors such as ionization chambers[3], or Geiger Mueller detector[6] as well as solid-state detectors such as scatter probes[5]. These measurements can be made using acrylic phantoms in experimental setups, in real clinical environments, or through computational simulations[7,8].

In practice, it is often impractical to place radiation-measuring devices throughout a hospital ward due to space limitations and the high patient occupancy. Therefore, in this study, we aimed to measure the scattered radiation levels around mobile CXR units at various positions in a controlled laboratory environment. The dose data we collected were used to estimate the exposure to scattered radiation of health care personnel, including nurses and other individuals who may be present in the patient rooms during CXR examinations.

METHODS

Because this study did not involve human participants, the Institutional Review Board of the Faculty of Medicine Vajira Hospital granted an exemption (exemption No. COE: 030/2023X), specifically pertaining to the use of phantoms and simulated radiation measurements.

We placed an adult anthropomorphic phantom (PBU-50, Kyoto Kagaku Co., Ltd, Japan) on a bed in a semi-upright position to simulate an anteroposterior CXR procedure. The X-ray tube was positioned 100 centimeter (cm) from the image receptor, with exposure parameters set to 80 kilovoltage peak (kVp) and 2 mAs. To measure the scattered radiation dose, we used a 100-centimeter square (cm^2) RTI scatter probe (RTI Group, Mölndal, Sweden). The probe was calibrated by the manufacturer according to ISO standards, with a measurement accuracy of ± 10% or ± 0.3 microgray per hour (μGy/h). For consistency, the probe was mounted on a tripod at a height of 80 cm above the floor (representing the level of reproductive organs for an average adult male height of 175 cm). The radiation doses were measured at distances of 1.0, 1.5, and 2.0 meters (m) from the phantom's centerline, at angles of 0°, 45°, 90°, 135°, 180°, 225°, 270°, 315°, and 360° relative to the central axis (Figure 1). We recorded both air kerma (μGy) and air kerma rate (μGy/h). To ensure accuracy and account for variability, each measurement was repeated three times at every distance and angle.

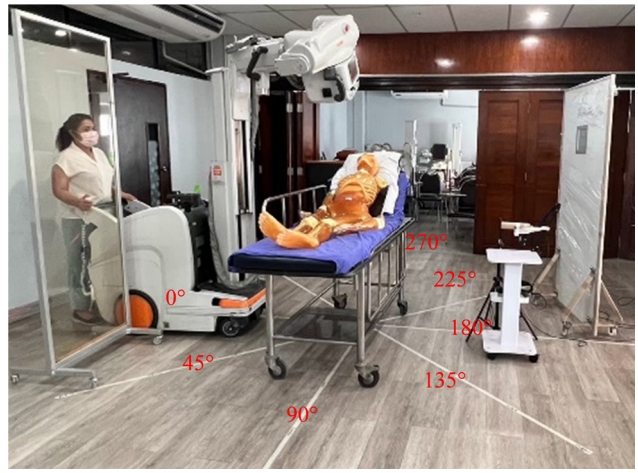


Figure 1 Experimental setup for measuring scattered radiation during chest X-ray imaging using a mobile X-ray unit

To simulate chest imaging of a pediatric patient in a supine position, we used a 10-cm thick acrylic sheet to approximate the body thickness of the pediatric patient. The exposure parameters were set to 55 kVp and 1.6 mAs to reflect the lower dose typically used in pediatric imaging. The source-to-image distance (SID) was maintained at 100 cm. Consistent with the adult protocol, the RTI scatter probe was positioned at a height of 80 cm from the ground. The radiation doses were measured at distances of 1.0, 1.5, and 2.0 m, using the same angular positions used in the adult measurements. Based on the consistency of the results obtained from the adult phantom, only one measurement per distance and angle was performed in the pediatric setup to confirm the radiation distribution trend and to reduce unnecessary repetition.

We conducted a quantitative analysis of all collected data. The maximum and minimum radiation doses recorded at each distances and angles were calculated. We used the mean values and standard deviations (SD) to summarize the central tendency and variability of the measurements. The results were presented in tables to illustrate the distribution of the scattered radiation around the mobile X-ray unit.

We estimated the scattered radiation doses in hospital wards using detailed floor plans and actual room dimensions. Comprehensive information on room materials, medical equipment, and patient bed locations was collected to ensure simulation accuracy. To enable precise spatial analysis, we used SketchUp software to model the ward layouts. The exposure of staff and patients in adjacent beds to radiation was evaluated under three simulation scenarios. In the first scenario, which assumed an open space without walls or partitions, we applied the inverse square law using a reference point 1 m from the X-ray source (point A), and calculated the scattered dose at a secondary point (point B) accordingly (Figure 2a). In the second scenario, in which the measured distances and angles from the X-ray machine matched the experimental setup (i.e., 1.0, 1.5, or 2.0 m), we assumed the radiation dose at point A to be equal to the experimentally measured value at the corresponding distance (Figure 2b). In the third scenario, which involved walls or shielding partitions, we initially applied the inverse square law from a 1-m reference point, followed by the Lambert Beer law to calculate the attenuation of radiation through materials. The resulting attenuated value was then used in a second inverse square law calculation to estimate the dose at point C (Figure 2c). The linear attenuation coefficients used in the simulations were 0.28 cm^{-1} for acrylic glass[9], 0.66 cm^{-1} for plate glass [9], 0.127 cm^{-1} for wood [10], 0.136 cm^{-1} for aluminum [11], and 1.45 cm^{-1} for concrete[12].

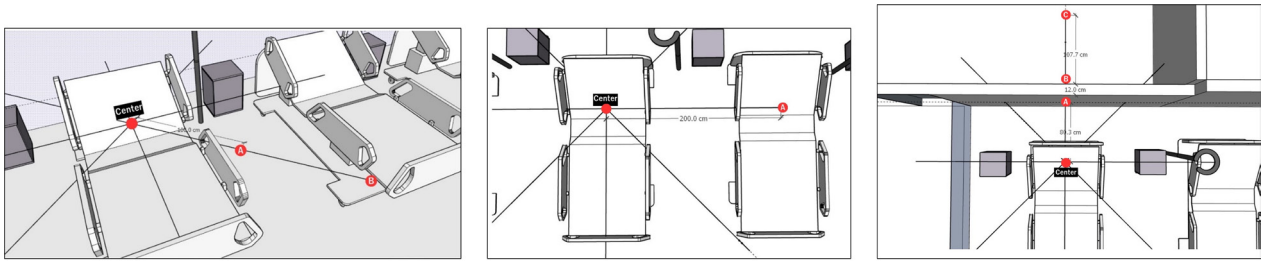


Figure 2 Estimation of scattered radiation doses received by staff and adjacent patient beds under three scenarios: (a) without walls or partitions; (b) with measured distances; and (c) with walls or partitions

RESULTS

We measured the scattered radiation values around the mobile X-ray unit using an adult phantom at distances of 1.0, 1.5, and 2.0 m from the X-ray tube, and at angles of 0°, 45°, 90°, 135°, 180°, 225°, 270°, 315°, and 360° relative to the central axis. The exposure parameters were set to 80 kVp and 2 mAs, with an SID of 100 cm. The variability in scattered radiation values is presented as mean ± SD in Table 1, reflecting the reproducibility of repeated measurements. These error estimates demonstrate consistency across most positions, with slightly higher variability observed at angular positions where scatter was less uniform. We observed the highest scattered radiation dose at a distance of 1.0 m, with an average air kerma of 0.26 µGy at angles of 0°, 45°, and 180°, primarily adjacent to the patient's bed. In contrast, the lowest dose, with a value of 0.03 µGy, was recorded at the head side of the bed (270°). Radiation values consistently decreased as distance increased (Table 1).

We conducted scattered radiation measurements using the pediatric phantom at distances of 1.0, 1.5, and 2.0 m from the X-ray tube, using the same nine angular positions as in the adult setup. The exposure parameters were set to 55 kVp and 1.6 mAs, and the results are included in Table 1. We recorded the highest scattered dose at 45° and 1.0 m, measuring 0.107 µGy. In contrast, the lowest dose occurred at 270° and 2.0 m, with a value of 0.002 µGy.

Table 1 Measured scattered radiation dose (in µGy) at varying distances (1.0 m, 1.5 m, and 2.0 m) from the X-ray source using adult and pediatric phantoms. Values represent the mean of three measurements ± SD.

			Adult CXR (80 kVp and 2 mAs)			Pediatric CXR (55 kVp and 1.6 mAs)	
No.	Angle (Degrees)	Distance (meter)	Air kerma rate	Air kerma (µGy)		Air kerma rate	Air kerma
			(mGy/h)	Average	SD	(mGy/h)	(µGy)
1	0, 360	1.0	48.44	0.26	0.01	0.01	0.036
2	0, 360	1.5	43.62	0.18	0.00	4.47	0.019
3	0, 360	2.0	23.49	0.10	0.00	2.51	0.010
4	45	1.0	54.20	0.26	0.04	26.33	0.107
5	45	1.5	38.72	0.17	0.01	7.94	0.038
6	45	2.0	19.89	0.08	0.00	2.78	0.018
7	90	1.0	N/A	N/A	N/A	N/A	N/A
8	90	1.5	6.39	0.04	0.00	5.17	0.027
9	90	2.0	7.04	0.04	0.01	3.48	0.015

Table 1 Measured scattered radiation dose (in μGy) at varying distances (1.0 m, 1.5 m, and 2.0 m) from the X-ray source using adult and pediatric phantoms. Values represent the mean of three measurements ± SD. (continued)

			Adult CXR (80 kVp and 2 mAs)			Pediatric CXR (55 kVp and 1.6 mAs)	
No.	Angle (Degrees)	Distance (meter)	Air kerma rate	Air kerma (μGy)		Air kerma rate	Air kerma
			(mGy/h)	Average	SD	(mGy/h)	(μGy)
10	135	1.0	35.77	0.23	0.12	16.69	0.070
11	135	1.5	31.94	0.18	0.01	6.70	0.028
12	135	2.0	20.13	0.10	0.00	3.84	0.016
13	180	1.0	47.72	0.26	0.02	6.82	0.031
14	180	1.5	37.44	0.18	0.01	4.10	0.017
15	180	2.0	22.06	0.11	0.00	1.53	0.010
16	225	1.0	35.38	0.24	0.01	3.57	0.015
17	225	1.5	29.03	0.12	0.00	1.72	0.008
18	225	2.0	15.85	0.08	0.00	1.08	0.005
19	270	1.0	6.56	0.03	0.00	2.15	0.008
20	270	1.5	13.84	0.07	0.01	0.97	0.004
21	270	2.0	9.99	0.04	0.00	0.05	0.002
22	315	1.0	21.80	0.10	0.08	3.88	0.016
23	315	1.5	29.93	0.13	0.00	2.13	0.008
24	315	2.0	18.55	0.08	0.01	1.07	0.005

Abbreviations: CXR, chest X-ray; h, hour; kVp, kilovoltage peak; mAs, milliampere-seconds; mGy, milligray; SD, standard deviation; μGy, microgray
"N/A" denotes "Not Applicable," indicating areas where data could not be collected due to issues with the scatter probe installation.

We used the floor plan of the adult patient ward to estimate the scattered radiation doses at key locations during the mobile X-ray procedures (Figure 3). In the isolation room, scattered radiation reached adjacent beds at angles of 270° and 180°, with calculated doses of 0.013 μGy and 0.042 μGy, respectively. For the standard patient bed location, we found that scattered radiation affected both the left and right adjacent beds, particularly at angles of 0°, 45°, 135°, and 180°. The estimated doses were approximately 0.153 μGy on the right side and 0.154 μGy on the left side. At the nurse's station, which was located near another patient bed, the scattered radiation reached the work area at 45°, 90°, 135°, and 180°, with a calculated dose of approximately 0.04 μGy.

We also used the pediatric ward layout to estimate the scattered radiation levels under clinical scenarios (Figure 3). At nurse station 1, scattered radiation reached the work area at angles of 45°, 90°, and 135°, resulting in a cumulative dose of 0.051 μGy. At nurse station 2, radiation exposure occurred at angles of 225° and 270°, with a much lower estimated dose of 0.001 μGy. In the area between the adjacent patient beds, scattered radiation again reached the nurse's station at 45°, 90°, and 135° angles, with a total dose of 0.051 μGy. In addition, we measured radiation at the adjacent beds themselves, with estimated doses of 0.016 μGy at 0° for the bed on the right and 0.014 μGy at 180° for the bed on the left.

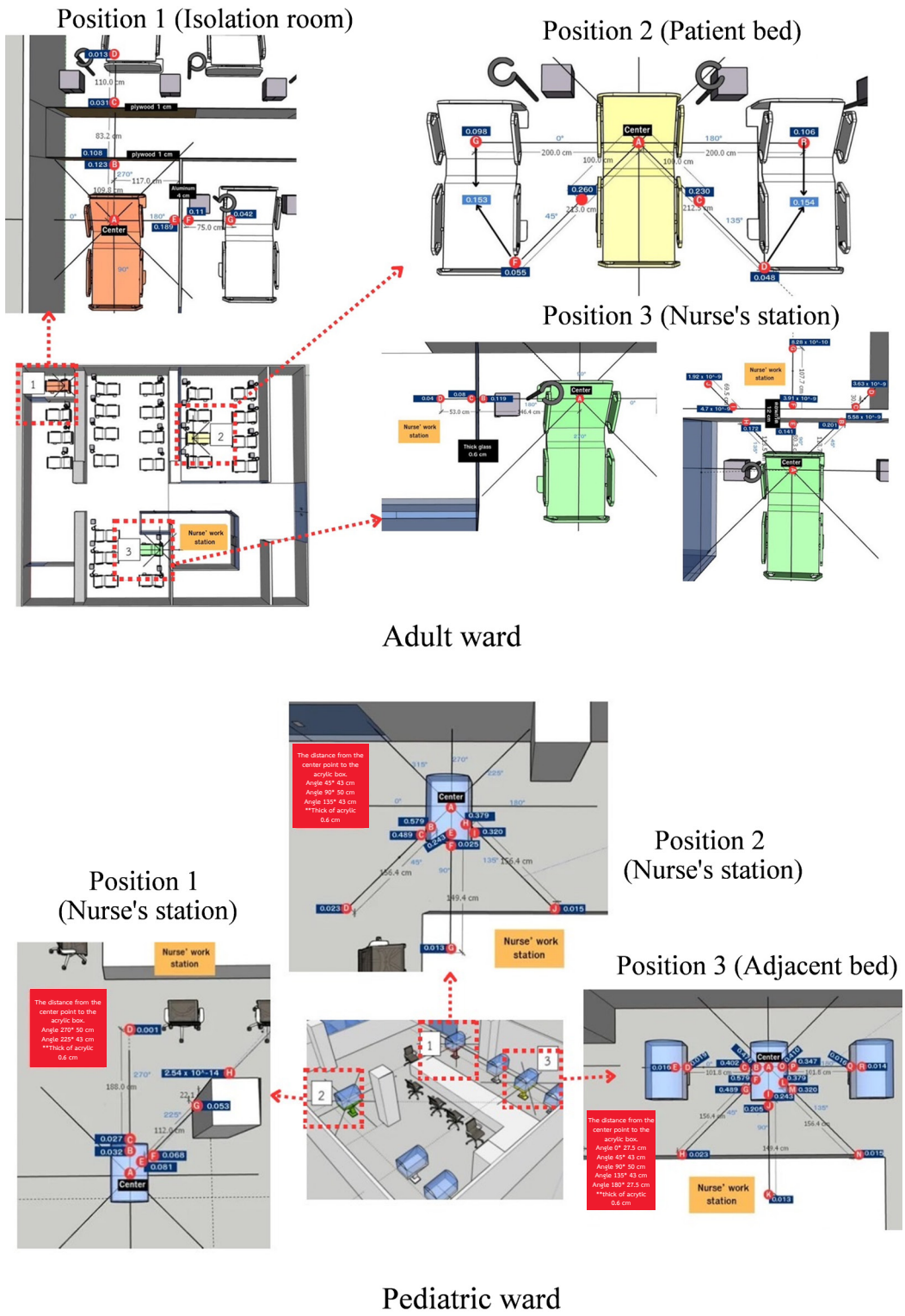


Figure 3 Floor plans of the adult ward (top) and pediatric ward (bottom), illustrating scattered radiation dose calculations (μGy) based on X-ray imaging positions and surrounding bed and nurse station locations

We evaluated the annual radiation exposure resulting from the use of mobile X-ray units in hospital wards in relation to the dose limits recommended by the International Commission on Radiological Protection (ICRP)[13]. The ICRP sets an annual dose limit of 1 millisievert (mSv) for the general public, a standard that applies to both patients in adjacent beds and health care workers who are routinely present in the ward environment. Based on an estimated frequency of two CXR examinations per bed per day, we calculated the annual number of exposures per bed to be approximately 730. The results indicate that, under these usage conditions, the cumulative radiation doses received by nearby patients and health care personnel remained well below the 1 mSv threshold, as detailed in Tables 2 and 3. These findings support the safety of routine mobile radiography in inpatient settings when appropriate protocols and distancing measures are followed.

Table 2 Estimated annual scattered radiation dose (in mSv) to adjacent patients and healthcare workers in the adult ward, based on 730 chest radiography sessions per year. Values were calculated using measured scattered radiation data and simulated ward layouts.

The location where the X-ray is performed	Angle (degrees)	Area receiving radiation	Radiation dose calculated per exposure (μSv)	Radiation dose per year (mSv)
Isolation room	270	adjacent bed 1	1.3×10^{-2}	9.3×10^{-3}
	180	adjacent bed 2	4.2×10^{-2}	3.1×10^{-2}
Observation bed	0	adjacent bed 3	9.8×10^{-2}	7.2×10^{-2}
	45	adjacent bed 3	5.5×10^{-2}	4.0×10^{-2}
	135	adjacent bed 4	4.8×10^{-2}	3.5×10^{-2}
	180	adjacent bed 4	1.1×10^{-1}	7.7×10^{-2}
Patient bed near the nurse's station	45	nurse workstation	3.6×10^{-9}	2.7×10^{-9}
	90	nurse workstation	8.3×10^{-10}	6.1×10^{-10}
	135	nurse workstation	1.9×10^{-9}	1.4×10^{-9}
	180	nurse workstation	4.0×10^{-2}	2.9×10^{-2}

Abbreviations: mSv, millisievert; μSv, microsievert

Table 3 Estimated annual scattered radiation dose (in mSv) to adjacent patients and healthcare workers in the pediatric ward, based on 730 chest radiography sessions per year. Values were calculated using measured scattered radiation data and simulated ward layouts.

The location where the X-ray is performed	Angle (degrees)	Area receiving radiation	Radiation dose calculated per exposure (μSv)	Radiation dose per year (mSv)
Patient bed near the nurse's station 1	45	nurse workstation	2.3×10^{-2}	1.7×10^{-2}
	90	nurse workstation	1.3×10^{-2}	9.5×10^{-3}
	135	nurse workstation	1.5×10^{-2}	1.1×10^{-2}
Patient bed near the nurse's station 2	225	nurse workstation	2.5×10^{-14}	1.8×10^{-14}
	270	nurse workstation	1.0×10^{-3}	7.3×10^{-4}
Between patient bed	0	adjacent bed 1	1.6×10^{-2}	1.2×10^{-2}
	45	nurse workstation	2.3×10^{-2}	1.7×10^{-2}
	90	nurse workstation	1.3×10^{-2}	9.5×10^{-3}
	135	nurse workstation	1.5×10^{-2}	1.1×10^{-2}
	180	adjacent bed 2	1.4×10^{-2}	1.0×10^{-2}

Abbreviations: mSv, millisievert; μSv, microsievert

DISCUSSION

Scattered radiation levels measured in this study consistently decreased with increasing distance from the radiation source, in line with the inverse square law. This pattern was observed for both adult and pediatric phantom setups, confirming that distance remains the most effective factor in reducing scatter exposure. Although radiation doses were generally low, the measurements also showed variability across angles, reflecting the non-uniform distribution of scatter around the patient and X-ray tube.

In the adult ward simulations, scattered radiation reached adjacent beds and nurse workstations, with certain positions receiving higher exposure than others. These estimates provide insight into the spatial distribution of scattered radiation and help identify areas where exposure control may be most critical. In pediatric ward conditions, radiation levels remained lower overall; however, the proximity and orientation of patients and staff to the X-ray source still resulted in measurable exposure. These findings highlight the importance of considering clinical ward layouts when planning radiation protection strategies.

Scattered radiation around a mobile X-ray machine during CXR imaging can be measured using either a physical phantom[5] or computational simulation such as the Monte Carlo method with the Particle and Heavy Ion Transport code System[7]. Scattered radiation exhibits uncertain and non-uniform directional patterns. Using a phantom with a radiation detector enables practical data collection through relatively straightforward procedures; however, it requires measurements from multiple positions surrounding the X-ray source. In contrast, Monte Carlo simulations—although more complex—offer a more comprehensive assessment of the spatial distribution and probability of scattered radiation as compared with phantom-based methods.

The spatial variability of scattered radiation requires the use of appropriate detectors to assess radiation levels across different cross-sectional areas. Survey meters, which use gas-filled detectors for air ionization, are portable, highly sensitive to moderate-to-high radiation levels, and can provide accurate readings across a broad range. However, these instruments measure radiation omnidirectionally (from both the front and sides), which makes it difficult to determine the exact direction of the scattered radiation. Survey meters are particularly suitable for environments with radioactive sources and for occupational radiation monitoring. In contrast, a scatter probe is a solid-state (semiconductor) detector specifically designed to measure scattered or leakage radiation. It has a flat, one-sided detection surface that enables directional detection, minimizing the interference from off-axis radiation. This design allows for more accurate and precise measurements of low-dose scattered radiation. Therefore, the choice of detector is critical to ensure the accurate assessment of scattered radiation in clinical environments.

Scattered radiation generally decreases with increasing distance from the X-ray source, which is consistent with the inverse square law, that states that the intensity of radiation decreases proportionally to the square of the distance. However, we noted exceptions at certain positions, such as the head of the patient's bed, where the measured radiation at 1 m was lower than that at 1.5 m. This anomaly may be attributed to the directional nature of the scatter, probe orientation, and attenuation caused by the bed structure or surrounding materials. Such factors can lead to deviations from the theoretical model.

Scattered radiation levels were higher in the adult ward as compared with the pediatric ward due to the greater patient body thickness of the adults and the use of greater technical factors in adult imaging. This increase in scatter corresponds with the shift from photoelectric absorption to Compton scattering at higher kVp settings. These findings are consistent with previous studies by Tam et al.[5] and Renger et al.[14], who demonstrated that the scattered radiation increases with higher tube potential.

In this study, we applied the Lambert Beer attenuation equation and the inverse square law to assess the distribution of radiation across hospital wards. To estimate the potential exposure received by adjacent patients and health care workers, we obtained the reference doses from actual measurements. Assuming the use of mobile X-ray twice per day per bed (approximately 730 times per year), the estimated scattered radiation doses remained well below the ICRP's recommended public exposure limit of 1 mSv per year. These findings are in agreement with the reports by Moonkum et al.[4] and Chiang et al.[3], who reported that radiation levels beyond 2 m fall to near-background values. Although the measured radiation doses in this study were well below the deterministic thresholds, there remains a theoretical risk of stochastic effects from cumulative exposure over time.

This study has several strengths. It included both adult and pediatric phantoms, allowing comparison under two relevant clinical conditions. Systematic measurements at different distances and angles, together with the use of a calibrated scatter probe, provided reliable low-dose data. The integration of measurements with ward simulations further enhanced the practical value of the findings by reflecting real hospital settings. However, some limitations should be noted. Only one adult and one simplified pediatric phantom were used, which may not represent the full range of patient anatomies. The study was performed with a single mobile X-ray unit and limited exposure protocols, and scatter was measured only at selected positions and heights. Ward simulations relied on specific floor plans and material assumptions, which may differ from real environments. Moreover, the controlled setup did not account for clinical factors such as staff movement, patient variability, or repeated exposures. Future studies should include a wider range of mobile X-ray units, diverse ward environments, and phantoms of varying sizes, and may benefit from simulation techniques such as Monte Carlo methods to provide more comprehensive, three-dimensional assessments of scatter distribution and risk.

Future studies should consider evaluating a broader range of mobile X-ray machines and expanding the measurements to include more diverse hospital environments. Because scattered radiation is influenced by patient anatomy and body size, future research should include phantoms of various sizes to improve the generalizability of the findings. We used a single phantom model in this study, which limits its applicability to the full range of patient populations. In additional, although we measured scattered radiation at multiple angles and distances, it was not possible to capture all directions of the scattered radiation emission. Future studies using simulation techniques, such as Monte Carlo methods, may provide more complete and three-dimensional assessments of the distribution and risk of scatter.

CONCLUSION

We found that the scattered radiation doses measured around a mobile X-ray machine during chest radiography using adult and pediatric phantoms at a distance of 1 m were within the recommended exposure limits for the general public. Although these levels are not sufficient to cause deterministic effects, they might still pose a potential risk of stochastic effects with long-term, repeated exposure. To minimize unnecessary exposure, radiologic technologists should consistently wear lead aprons, and other individuals—including patient relatives or caregivers—should maintain a minimum distance of 2 m from the X-ray unit during imaging procedures.

CONFLICT OF INTEREST

The authors declare no conflict of interest relevant to this study.

ACKNOWLEDGEMENT

The authors would like to express their sincere gratitude to the Faculty of Medicine Vajira Hospital for providing support and resources for this study. Special thanks are extended to the radiological technology team for their technical assistance during the experimental setup and data collection. The authors also confirm that no external funding was received for this work, and all expenses were personally covered by the authors.

DATA AVAILABILITY STATEMENT

The data supporting the findings of this study are available from the corresponding author upon reasonable request.

REFERENCES

1. Jacobi A, Chung M, Bernheim A, Eber C. Portable chest x-ray in coronavirus disease-19 (COVID-19): a pictorial review. Clin Imaging 2020;64:35-42.
2. Otomo K, Inaba Y, Abe K, Onodera M, Suzuki T, Sota M, et al. Spatial scattering radiation to the radiological technologist during medical mobile radiography. Bioengineering (Basel) 2023;10(2):259.
3. Chiang HW, Liu YL, Chen TR, Chen CL, Chiang HJ, Chao SY. Scattered radiation doses absorbed by technicians at different distances from X-ray exposure: Experiments on prosthesis. Biomed Mater Eng 2015;26 Suppl 1:S1641-50.
4. Moonkum N, Jitchom S, Sukaram S, Nimtrakool N, Boonrat P, Tochaikul G. Determination of scattered radiation dose for radiological staff during portable chest examinations of COVID-19 patients. Radiol Phys Technol 2023;16(1):85-93.
5. Tam SY, Fung YY, Lau SY, Lam WN, Wong ET. Scatter radiation distribution to radiographers, nearby patients and caretakers during portable and pediatric radiography examinations. Bioengineering (Basel) 2023; 10(7):779.
6. Onu CP, Nzotta CC. Scatter radiation levels in X-ray rooms during chest radiography. Appl Radiat Isot 2024;212:111472.
7. Abdul Aziz MZ, Yani S, Haryanto F, Ya Ali NK, Tajudin SM, Iwase H, et al. Monte Carlo simulation of X-ray room shielding in diagnostic radiology using PHITS code. J Radiat Res Appl Sci 2020;13(1):704-13.
8. Gonzales AC, Soares MR, Batista WOG, Cardeña AR, Marquez JP, Vega JR. Application of the Monte Carlo scattered radiation dose due to the use of handheld x-ray in dentistry. Radiat Prot Dosimetry 2022;198(16):1210-8.
9. Mamat N, Mohamad Tajudin S, Hanim Aminordin Sabri A, Faddilah Mohd Noor A, Norizan N, Zahri Abdul Aziz M. A comparative photon shielding properties of protective Window materials by using EGS5 code. IOP Conf Ser: Mater Sci Eng 2022;1231(1):012006.
10. Brown S, Bailey DL, Willowson K, Baldock C. Investigation of the relationship between linear attenuation coefficients and CT Hounsfield units using radionuclides for SPECT. Appl Radiat Isot 2008;66(9):1206-12.
11. Qadr HM. Calculation for gamma ray buildup factor for aluminium, graphite and lead. Int J Nucl Energy Sci Technol 2019;13(1):61-9.
12. Aziz F, Panitra M, Rivai AK. Synthesis and Monte Carlo simulation of improved concrete composites for enhanced x-ray/gamma ray radiation shielding. Int J Technol 2018; 9(4):291-319.
13. ICRP. The 2007 recommendations of the international commission on radiological protection [internet]. 2007 [cited 2024 Dec 30]. Available from: https://www.icrp.org/docs/icrp_publication_103-annals_of_the_icrp_37(2-4)-free_extract.pdf
14. Renger B, Brieskorn C, Toth V, Mentrup D, Jockel S, Lohöfer F, et al. Evaluation of dose reduction potentials of a novel scatter correction software for bedside chest x-ray imaging. Radiat Prot Dosimetry 2016; 169(1-4):60-7.